Fluid-Structure Interaction in the case of filaments:
Part 1: applications to passive control
Part 2: retinal detachment in the human eye.

Jan O. Pralits

Department of Civil, Chemical and Environmental Engineering
University of Genoa, Italy
jan.pralits@unige.it

October 19, 2015

The work in part 1 has been carried out in collaboration with:

- **Damiano Natali** DICCA, University of Genoa, Italy
- **Andrea Mazzino** DICCA, University of Genoa, Italy
- **Shervin Bagheri** KTH, Stockholm, Sweden
- **Franco Auteri** Politecnico di Milano, Italy
- **Eleonora Piersanti** Politecnico di Milano, Italy

Motivation

Here we study the dynamics of flexible, inextensible and massive filaments (permeable and impermeable), similar to the well-know flag problem.

What are the applications of such study?

- Paper processing
- Energy harvesting
- Turbulence control, flight control
- Behaviour of biological structures, such as leaves, in windy environments
- Locomotion of animals

... to just mention of few.

A fluid-structure interaction problem

Two monks were arguing about the temple flag waving in teh wind. One said, "**The flag moves.**" The other said, "**The wind moves.**" They argued back and forth but could not agree. Hui-neng, the sixth Patriarch, said: "Gentlemen! It is not the flag that moves. It is not the wind that moves. **It is your mind that moves.**" The two monks were struck with awe.

How has this problem been studied?

Experimental studies:
- Study of flags made of various fabrics and shapes hanging in a vertical wind tunnel
- Flexible filament made of silk thread and immersed in a running soap film
- Heavy, streamlined, and elastic body interacting with a fluid in a water tunnel
- Paper flutter: a potentially destructive phenomenon in high-speed printing

Inviscid simulations:
- Flag allowed to shed a vortex sheet from its trailing edge
- Thin-airfoil theory approximation
- Small displacements, neglecting vortex shedding and neglecting the tension

Viscous simulations: FSI DNS
- Immersed boundary (IB) method
- ALE finite-element method

Observed behaviours

Let us focus on the two-dimensional case

Movie 1
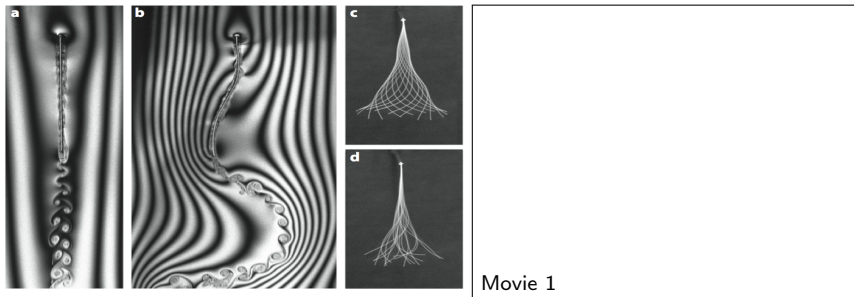
a) The stretched-straight state,
b) Flapping,
c) Coherent periodic flapping,
d) Aperiodic flapping ($\sim$ chaotic)

Linear stability- & sensitivity analysis
of
an impermeable filament

The aim of this analysis

For a viscous coupled problem where the structure has a rigidity, mass and is thin (filament), study:

- Linear stability (global modes)
- Structural sensitivity, Giannetti & Luchini (2007)
- To ascertain the role of the control parameters in the behaviour of the system, in particular the bifurcation curves.

The model

The dynamics of the flow is governed by the incompressible Navier-Stokes equations with suitable boundary conditions

$$\frac{\partial \mathbf{u}}{\partial t} + (\mathbf{u} \cdot \nabla)\mathbf{u} + \nabla p - \frac{1}{Re}\nabla \cdot (\nabla \mathbf{u} + \nabla \mathbf{u}^T) = 0, \tag{1}$$

$$\nabla \cdot \mathbf{u} = 0, \tag{2}$$

$$\left[p\hat{\mathbf{n}}_f - \frac{1}{Re}\nabla \cdot (\nabla \mathbf{u} + \nabla \mathbf{u}^T) \cdot \mathbf{n}_f \right]_{\Gamma_N} = 0, \tag{3}$$

$$\mathbf{u}|_{\Gamma_{in}} = \mathbf{u}_{in}, \tag{4}$$

$$\mathbf{u}|_{\Gamma_s} = \frac{\partial \mathbf{X}}{\partial t}, \tag{5}$$

where $\mathbf{n}_f$ is the outward pointing normal verso of the fluid domain. And the system of equations for the structure is given as

$$\frac{\partial^2 \mathbf{X}}{\partial t^2} = \frac{\partial}{\partial s}\left(\frac{1}{m}T\frac{\partial \mathbf{X}}{\partial s} \right) - \frac{\partial^2}{\partial s^2}\left(\gamma \frac{\partial^2 \mathbf{X}}{\partial s^2} \right) + \frac{\partial}{\partial s}\left(\gamma \left\| \frac{\partial^2 \mathbf{X}}{\partial s^2} \right\| \frac{\partial \hat{\mathbf{n}}}{\partial s} \right) + \frac{1}{m}\mathbf{F}, \tag{6}$$

$$\frac{\partial \mathbf{X}}{\partial s} \cdot \frac{\partial \mathbf{X}}{\partial s} = 1 \tag{7}$$

The force $\mathbf{F} = \mathbb{S}^+ \cdot \hat{\mathbf{n}}^+ + \mathbb{S}^- \cdot \hat{\mathbf{n}}^-$ is the difference in the fluid stress tensor between the upper (+) and lower (-) side of the filament, and $\mathbb{S} = -\nabla p + \frac{1}{Re}\nabla \cdot (\nabla \mathbf{u} + \nabla \mathbf{u}^T)$.

Non-dimensional parameters

The governing parameters of the problem are

- mass ratio: $m = \frac{\rho_s}{L\rho_0}$
- bending stiffness: $\gamma = \frac{EJ}{L^2 U_\infty^2 \rho_s}$
- Reynolds number: $Re = \frac{\rho_0 L U_\infty}{\mu}$

Verifying the code

The case analyzed here uses the following parameters:

Reduced velocity $U_s = K_b^{-0.5}$, with $K_b = m\gamma$ (Lee et al. (2014), Connell & Yue (2007), ...)
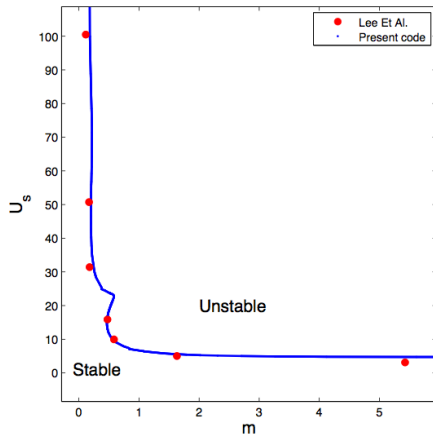
Reynolds number dependency

Increasing the Reynolds number there are two clear asymptotic behaviors.

However, for intermediate values of U_s and m the picture is less evident.
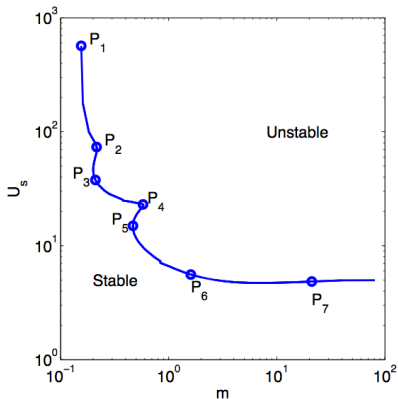
$Re = 200$, $\kappa = 10^6$
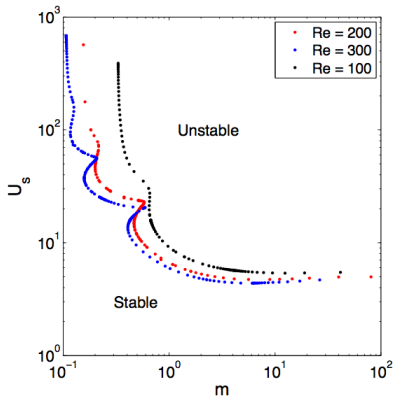
$Re = 100, 200, 300$, $\kappa = 10^6$

Critical values:
$U_s = 4.98$, $m_{Re=100} = 0.33$, $m_{Re=200} = 0.16$, $m_{Re=300} = 0.11$

A closer look at the eigenfunctions
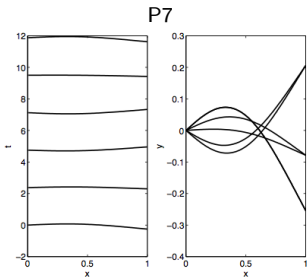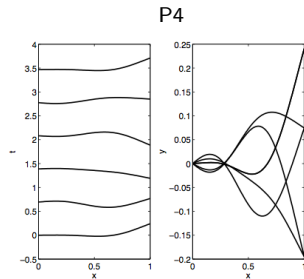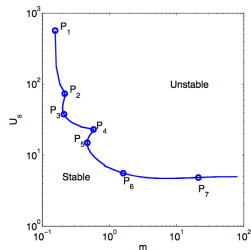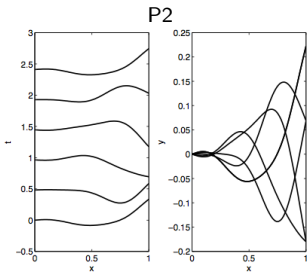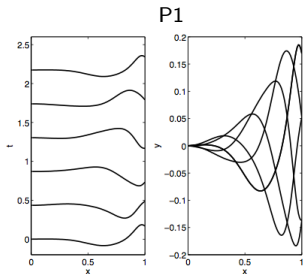
Direct & adjoint modes
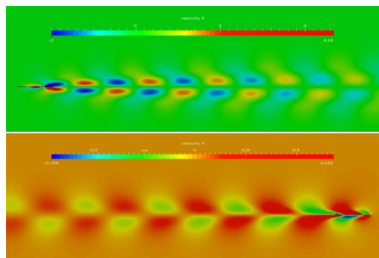
P_1
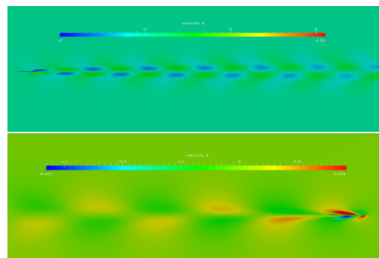
P_4
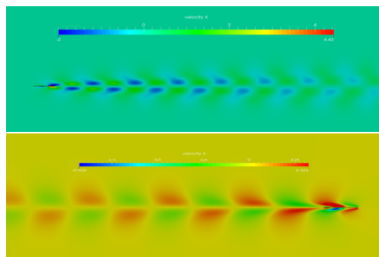
P_2
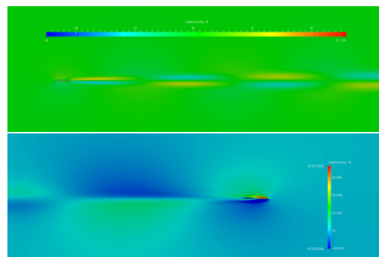
P_7

Structural sensitivity

P1

P2

P4

P7
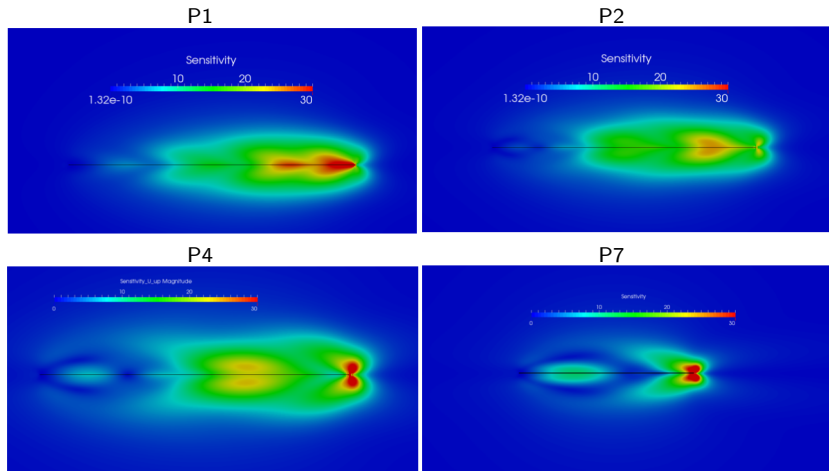
Conclusions

- A framework and numerical code has been set up, and verified, to perform LST, structural sensitivity (pseudo spectrum analysis, continuation method).
- For a given Reynolds number 2 asymptotic regimes are found (small bending stiffness/small mass SBM, high bending stiffness/high mass HBM). These regimes are related to hydrodynamic instabilities and structural instabilities, respectively.
- The structural sensitivity in the SBM case is a single region along the filament with a peak close to the trailing edge, while in the HBM case two distinct regions are found with the peak close to the trailing edge.
- For intermediate values of mass and bending stiffness "cusps" are found where **nodes** appear in the structure, and the position along the filament varies with the parameters. The nodes have zero vertical displacement during the flapping period.

P2   P4   neutral curve
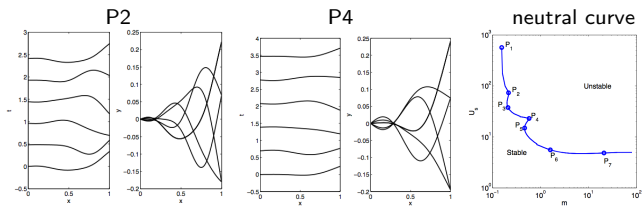
Porous filament

Motivations

The aim of the work is to explore numerically how different **structural parameters** (mass, bending stiffness and permeability) affect the dynamics of **biological tissues**, or **biomimetical surfaces** when exposed to **fluid flows**.
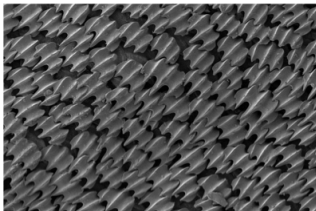
With such a study our objective is:

- to understand the underlying physics
- understand if there is a potential of porosity as a passive control device

Short on the state of the art

- Zhu and Peskin, Simulation of a Flapping Flexible Filament in a Flowing Soap Film by the Immersed Boundary Method (2002), **stretching and bending rigidity**.
- Kim and Peskin, 2-D Parachute Simulation by the Immersed Boundary Method (2006), **stretching rigidity and porosity**.
- Kim and Peskin, Penalty Immersed Boundary Method for an Elastic Boundary with Mass (2007), **stretching and bending rigidity and mass**.

In our model we introduce a filament with, simultaneously, **stretching and bending rigidity, porosity and mass**.

The FSI model
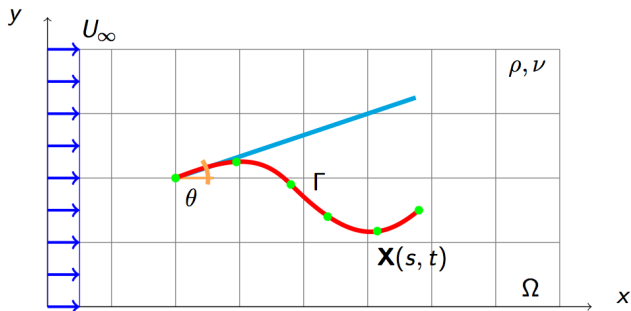
The filament Γ (in red) described by a set of Lagrangian points $\mathbf{X}(s, t)$ (in blue) immersed in the fluid domain Ω discretized by the Eulerian grid (in gray). The initial configuration (dotted line) of the filament is a straight line with a certain angle θ.

Governing equations

For the viscous incompressible fluid

$$\begin{cases} \dfrac{\partial \mathbf{u}}{\partial t} + \mathbf{u} \cdot \nabla \mathbf{u} = -\nabla p + \dfrac{1}{Re} \nabla^2 \mathbf{u} + \mathbf{f} \\ \nabla \cdot \mathbf{u} = 0 \end{cases}, \tag{8}$$

and for the 1D slender structure

$$\frac{\partial^2 \mathbf{X}}{\partial t^2} = \frac{\partial}{\partial s} \left(T \frac{\partial \mathbf{X}}{\partial s} \right) - \frac{\partial^2}{\partial s^2} \left(\gamma \frac{\partial^2 \mathbf{X}}{\partial s^2} \right) + Fr \frac{\mathbf{g}}{g} - \mathbf{F}, \tag{9}$$

$$\frac{\partial \mathbf{X}}{\partial s} \frac{\partial^2}{\partial s^2} \left(T \frac{\partial \mathbf{X}}{\partial s} \right) = \frac{1}{2} \frac{\partial^2}{\partial t^2} \left(\frac{\partial \mathbf{X}}{\partial s} \frac{\partial \mathbf{X}}{\partial s} \right) - \frac{\partial^2 \mathbf{X}}{\partial t \partial s} \frac{\partial^2 \mathbf{X}}{\partial t \partial s} - \frac{\partial \mathbf{X}}{\partial s} \frac{\partial}{\partial s} (\mathbf{F}_b - \mathbf{F}). \tag{10}$$

For the fluid we impose a constant velocity at the inlet, a convective condition at the outlet and symmetry condition in the cross-flow direction. The filament is hinged at the upstream point and conditions giving a free end is imposed at the trailing edge.

The following dimensionless parameters appear.

$$Re = \frac{U_\infty^* L^*}{\nu^*}, \quad Fr = \frac{g^* L^*}{U_\infty^{*2}}, \quad \rho = \frac{\rho_1^*}{\rho_0^* L^*}, \quad \gamma = \frac{K_b^*}{\rho_1^* U_\infty^{*2} L^{*2}}$$

How to model porosity?

Velocity-based approach by allowing a relative slip in the normal direction between the IB and the surrounding flow, given by:

$$\mathbf{u} = \mathbf{u}_{imp} + \lambda(\mathbf{F}_{imp} \cdot \mathbf{n})\mathbf{n} \tag{11}$$

This "classical" approach has a serious drawback since it uses the local (and often noisy) values of the force.

Forced-based approach by decreasing the force extert on the structure in the normal direction:

$$\mathbf{F} = (1 - \lambda) \cdot (\mathbf{F}_{imp} \cdot \mathbf{n})\mathbf{n} + (\mathbf{F}_{imp} \cdot \tau)\tau \tag{12}$$

With this approach the non-slip condition is obtained, to a certain accuracy, by using Goldstein's feedback rule

$$\mathbf{F}_{imp} = \alpha \int_0^t (\mathbf{U}_{ib} - \frac{\partial \mathbf{X}}{\partial t})dt' + \beta(\mathbf{U}_{ib} - \frac{\partial \mathbf{X}}{\partial t}), \tag{13}$$

where α and β are chosen such that the non-slip condition is enforced. Moreover, the velocity on the IB is computed as

$$\mathbf{U}_{ib}(s, t) = \int_\Omega \mathbf{u}(\mathbf{x}, t)\delta(\mathbf{x} - \mathbf{X}(s, t))d\Omega. \tag{14}$$

In a similar way the forcing of the Navier-Stokes equation is obtained as

$$\mathbf{f}(\mathbf{x}, t) = \rho \int_\Gamma \mathbf{F}(s, t)\delta(\mathbf{x} - \mathbf{X}(s, t))ds. \tag{15}$$

Benchmark using Darcy's law I
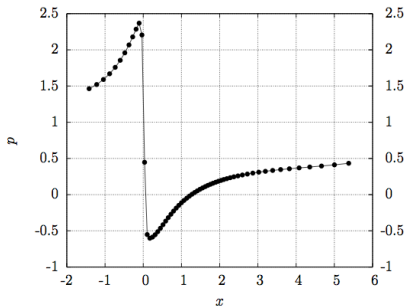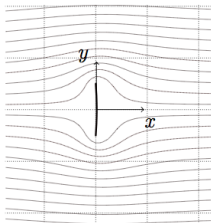
An inextensible membrane (left, thick solid line) simply supported at both ends is subject to a uniform flow from left (streamlines with thin solid lines) and (right) pressure profile along x. Notice the sudden pressure drop around membrane location (x = 0) within the space of two grid points.

Benchmark using Darcy's law II

Darcy's law $\mathbf{U}_{ib} - \frac{\partial \mathbf{X}}{\partial t} = -k_D \nabla p$

Goldstein's feedback law $\mathbf{F}_{imp} = \beta(\mathbf{U}_{ib} - \frac{\partial \mathbf{X}}{\partial t})$

Since the drag on a flat plate normal to the flow is only due to the pressure difference reduced by porosity one can assume that

$$\frac{\mathbf{F}_{imp}(1-\lambda)}{\delta} \sim \frac{\partial p}{\partial x},$$

where δ is the width of the membrane. This gives

$$k_D = -\frac{\delta}{\beta(1-\lambda)}$$
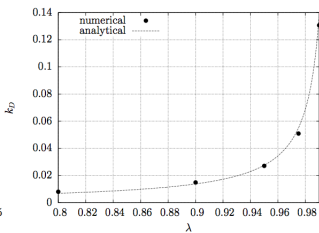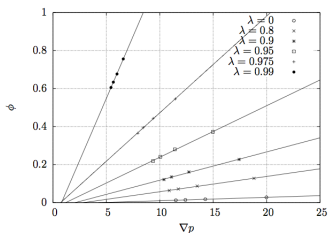
Validation with analytical model for impermeable filament

Connel & Yue (2007) proposed an analytical model based on slender body theory. It givens the following dispersion relation

$$(\rho + \rho_a)(1.3Re^{-0.5} + \gamma k^2) - \rho\rho_a \geq 0$$

where the added mass $\rho_a = 2/k$ comes from potential theory and k is the wave number associated with the filament shape when flapping.
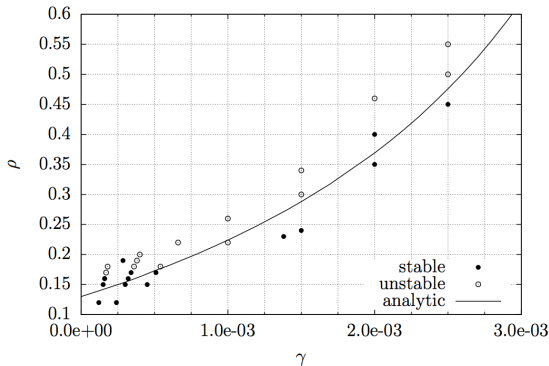
Comparison between analytical models and DNS simulations for Re $= 200$ and different values of ρ and γ.
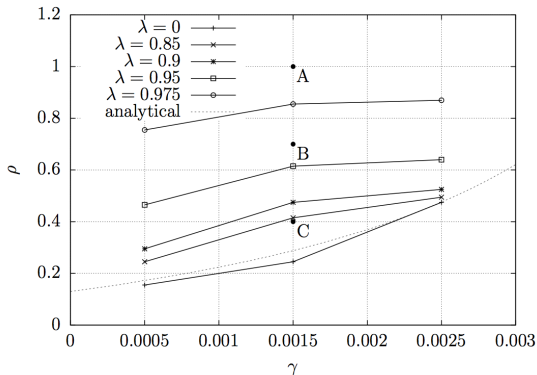
Porosity I

Neutral curve on the plane (γ, ρ) for $Re = 200$, $Fr = 0$ and $\lambda = 0$ obtained numerically. The analytical curve for $\lambda = 0$ is taken from Connel & Yue (2007) and shown with a dotted line, whereas the solid lines with symbols represent neutral curves for different porosity.

Note that large values of λ are needed for a "damping" effect.

Porosity II
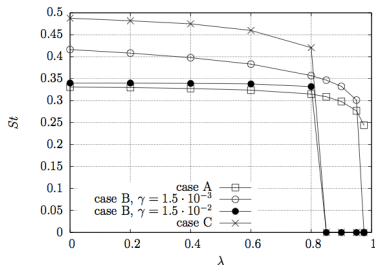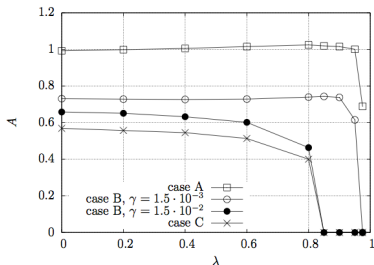
Peak-to-peak oscillation amplitude and flapping Strouhal number as function of porosity.

Clearly, "critical" values for λ, for which oscillations vanish, is close to unity. This can be estimated by comparing the characteristic time scales of porosity and hydrodynamical instabilities. We define the porous time scale τ_{por}^* as **the time it takes for the flow to reduce the pressure difference across the filament**. The hydrodynamical time scale is simply $\tau_{hdr}^* = L^*/U_\infty^*$. This gives an estimate of the critical porosity coefficient as

$$\lambda_{c,t} \approx 1 + \frac{\rho_a h}{\delta \beta}$$

Note that $\beta < 0$. Eg. Curve B ($\gamma = 1.5 \cdot 10^{-3}$): $\lambda_{c,n} = 0.95, \ \lambda_{c,t} = 0.91$.

Porosity III

Maximum values of lift and drag over a flapping period as a function of porosity (case C)
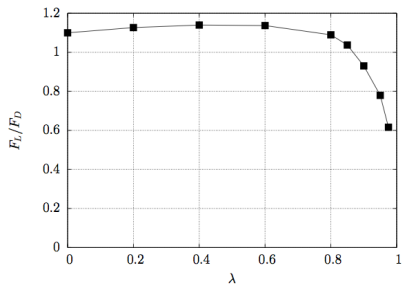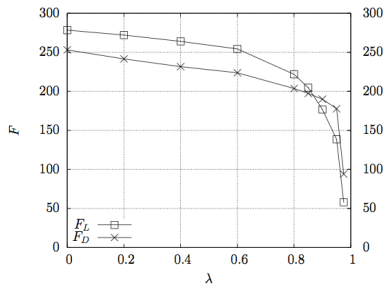
The lift/drag ratio is maximized for $\lambda \approx 0.6$

Conclusions

- A novel way of handling simultaneously porosity and bending resistance of a massive filament.
- It has been derived and verified a relation between the free model parameter λ and the porosity parameter k_D appearing in Darcys law and found that $k_D \sim (1 - \lambda)^{-1}$
- It is found that porosity effectively increases the stability zone only when the porosity parameter λ is greater that a critical value λ_c.
- We propose a simple resonance mechanism between a characteristics porous time-scale and the standard characteristic hydrodynamic time-scale, and the theoretical value is in qualitative agreement with the DNS simulations.
- We observed reduction of both lift and drag forces induced by porosity, ascribing it to the penetration velocity that reduces the pressure difference between the two sides of the structure, and find an optimum value of λ that maximizes the lift-to-drag ratio.